Electronic Supplementary Information for

Recycling decoration wastes toward a high-performance porous carbon membrane electrode for supercapacitive energy storage devices

Mengxia Cui,[a,b,c] Fang Wang,[a,b,c] Zhengguo Zhang,[a,b,c] Shixiong Min*[a,b,c]

[a] *School of Chemistry and Chemical Engineering, North Minzu University, Yinchuan, 750021, P. R. China.*

[b] *Key Laboratory of Chemical Engineering and Technology, State Ethnic Affairs Commission, North Minzu University, Yinchuan, 750021, P. R. China.*

[c] *Ningxia Key Laboratory of Solar Chemical Conversion Technology, North Minzu University, Yinchuan 750021, P. R. China.*

**Corresponding authors: sxmin@nun.edu.cn*

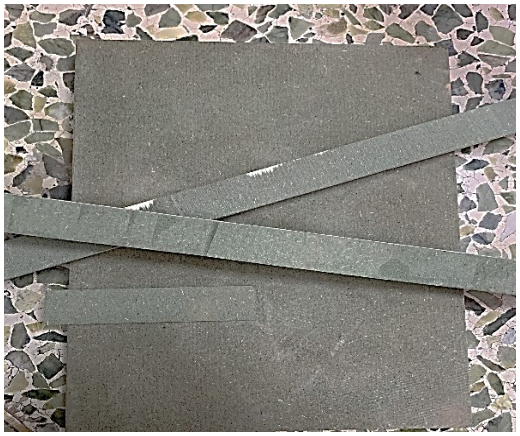

Fig. S1 The Digital photograph of wooden plastic plates.

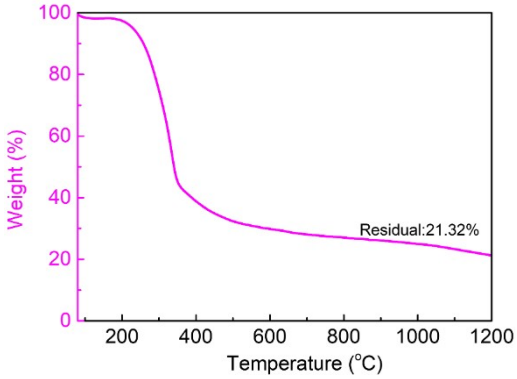

Fig. S2 TG curve of DWM-1-1000 electrode.

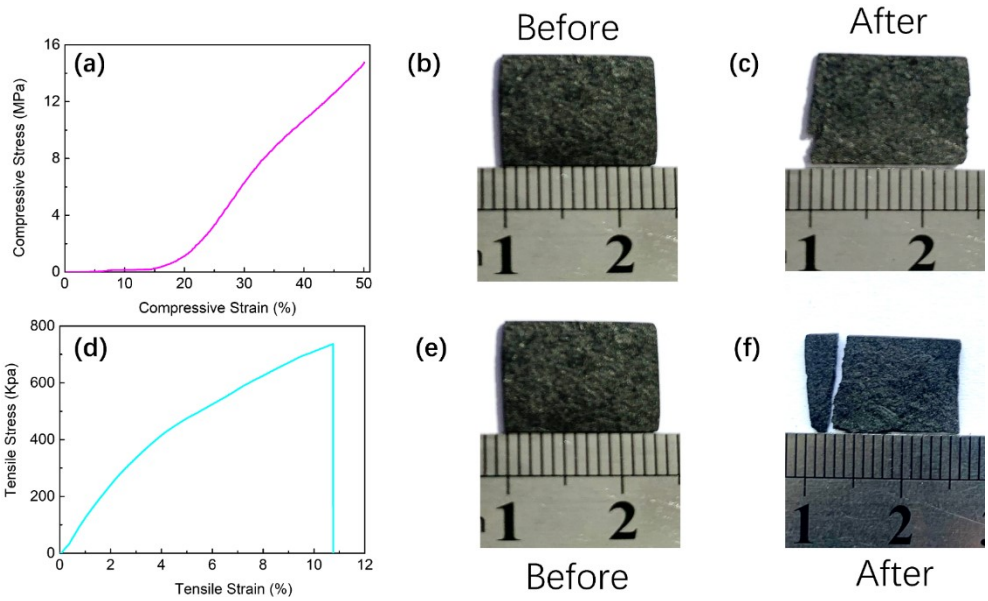

Fig. S3 (a) Compressive stress-strain curve of the DWCM-1-1000 electrode. (b) The digital photos of the DWCM-1-1000 electrode (b) before and (c) after compressive measurement. (d) Tensile stress-strain curve of DWCM-1-1000 membrane, and (e-f) digital images of DWCM-1-1000 electrode before and after tensile test.

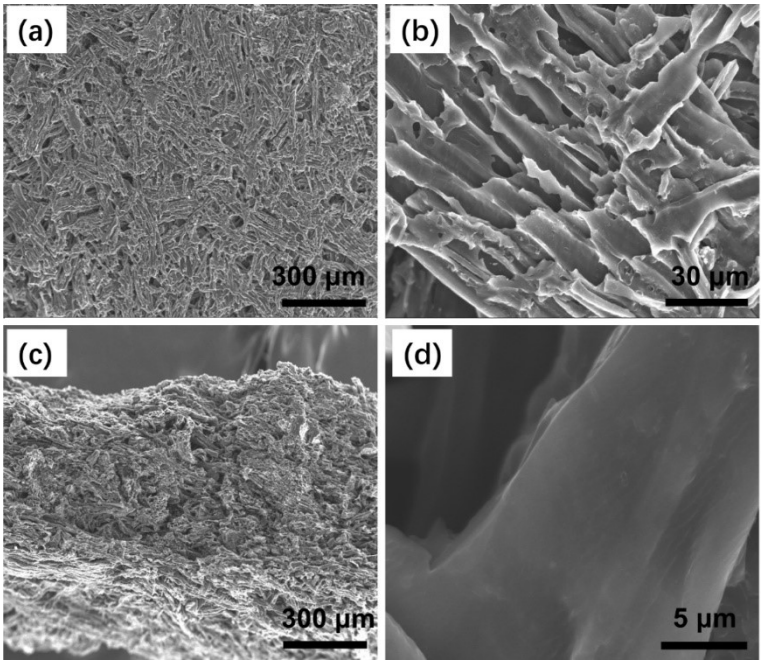

Fig. S4 (a, b) Top-view and (c, d) side-view SEM images of the DWCM-0-1000 electrode.

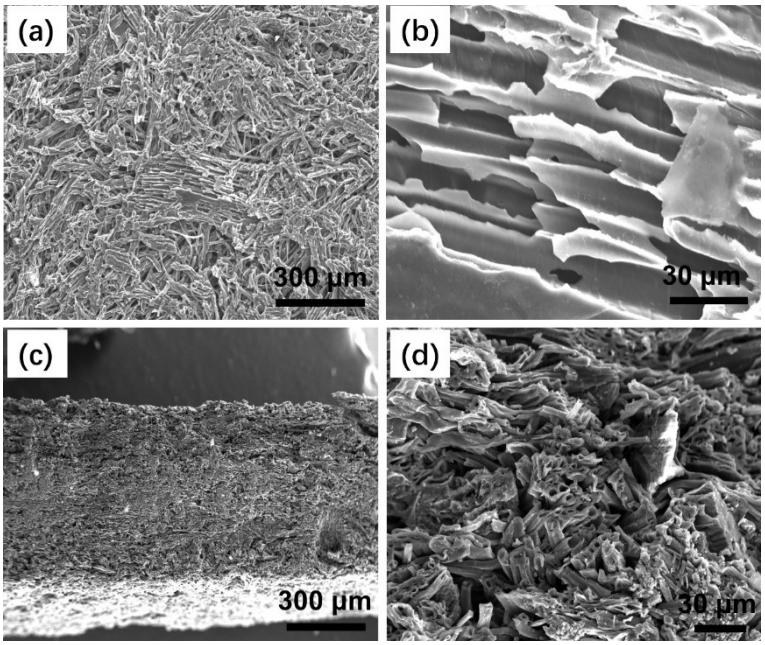

Fig. S5 (a, b) Top-view and (c, d) side-view SEM images of the DWCM-0.1-1000 electrode.

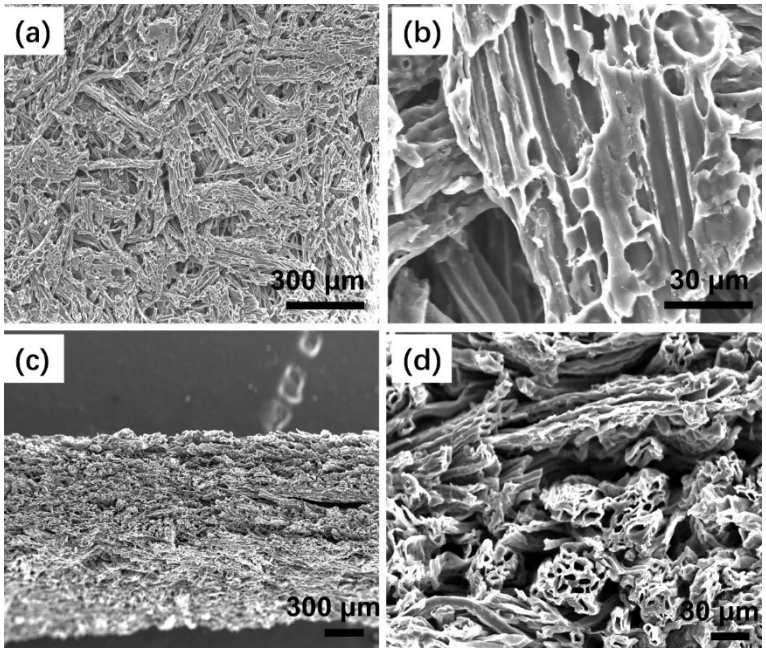

Fig. S6 (a, b) Top-view and (c, d) side-view SEM images of the DWCM-0.5-1000 electrode.

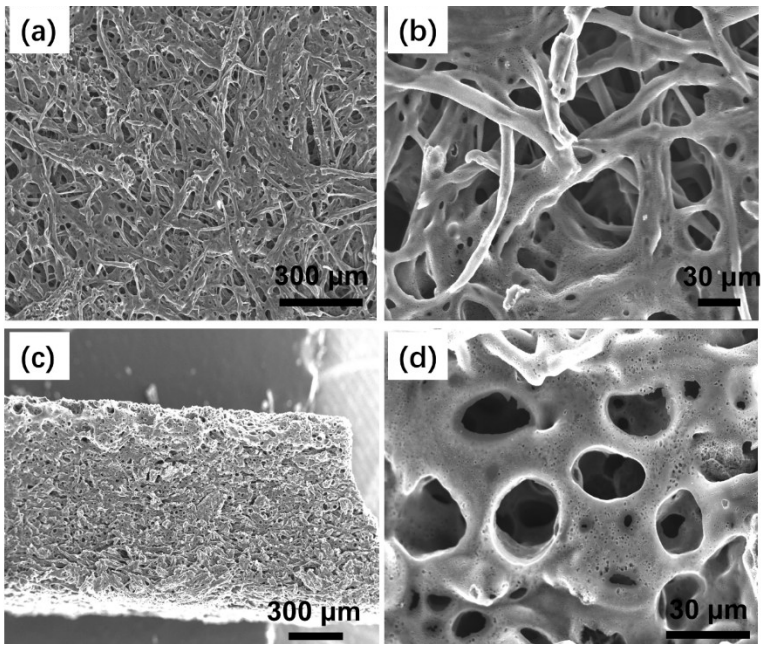

Fig. S7 (a, b) Top-view and (c, d) side-view SEM images of the DWCM-1-800 electrode.

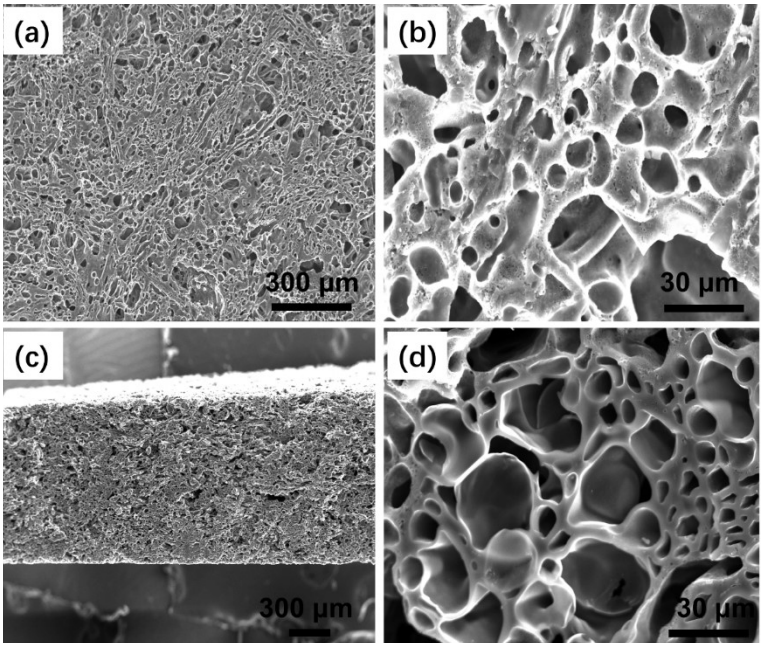

Fig. S8 (a, b) Top-view and (c, d) side-view SEM images of the DWCM-1-900 electrode.

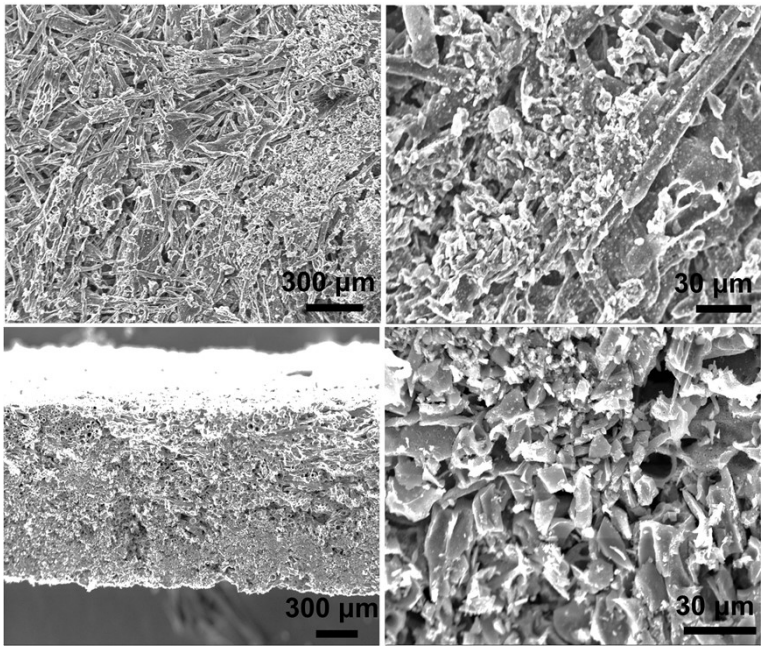

Fig. S9 (a, b) Top-view and (c, d) side-view SEM images of the DWCM-1-1100 electrode.

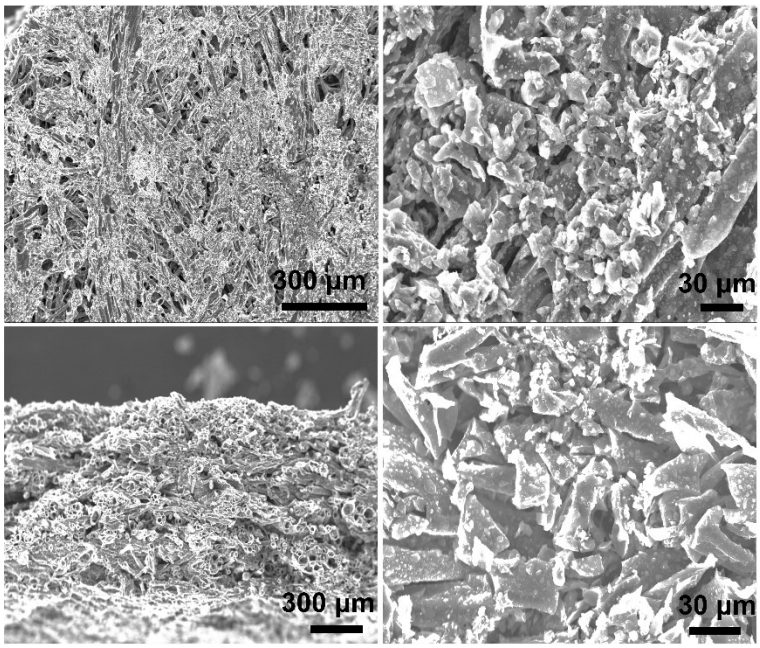

Fig. S10 (a, b) Top-view and (c, d) side-view SEM images of the DWCM-1-1200 electrode.

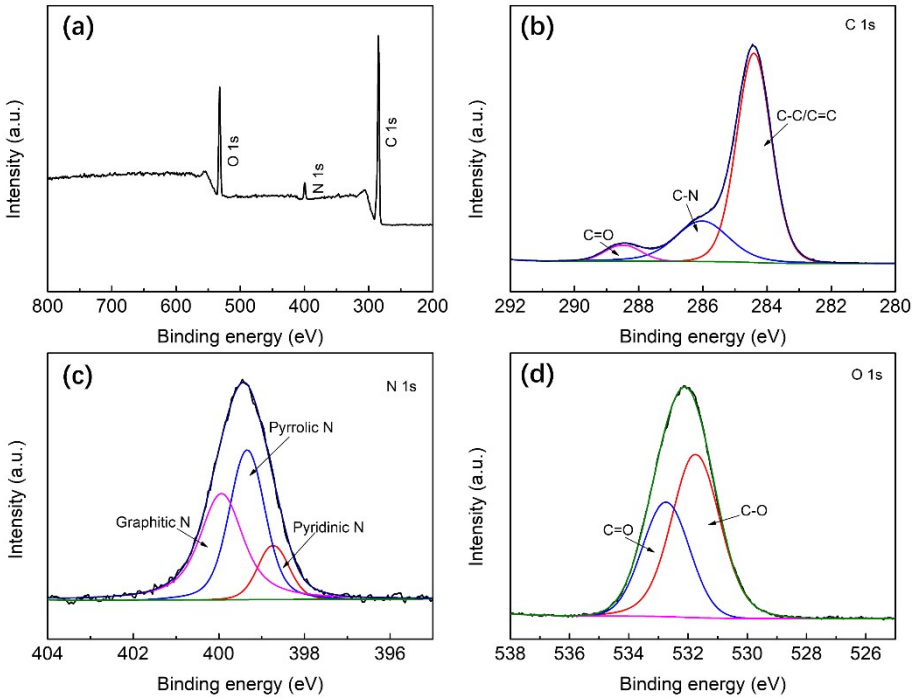

Fig. S11 (a) XPS survey spectra and high-resolution (b) C 1s, (c) N 1s, and (d) O 1s XPS spectra of the decoration waste (DW).

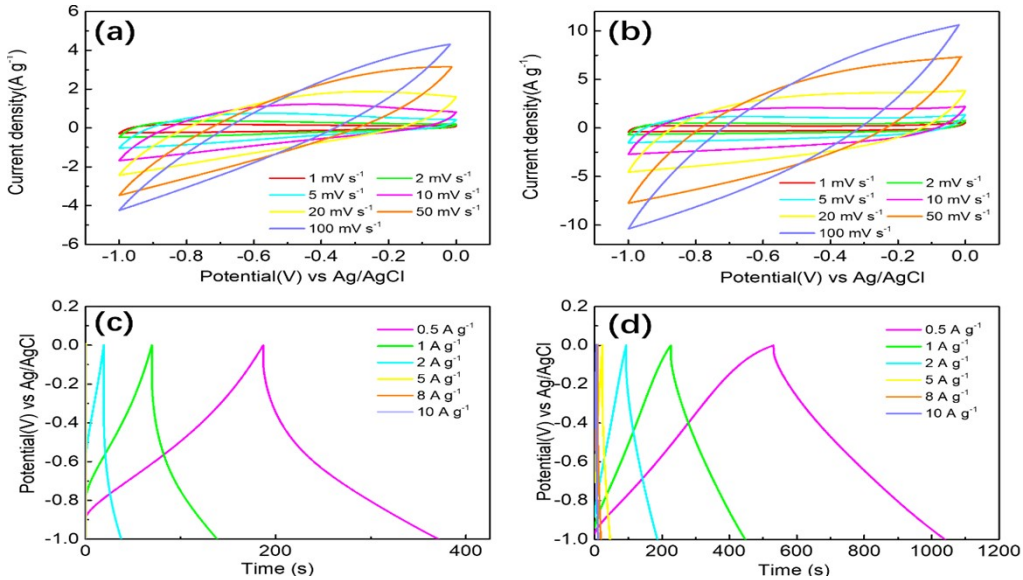

Fig. S12 CV curves of (a) DWCM-0.1-1000 electrode, (b) DWCM-0.5-1000 electrode in 6 M KOH solution at different scan rates. GCD curves of (c) DWCM-0.1-1000 electrode, (d) DWCM-0.5-1000 electrode at different current densities.

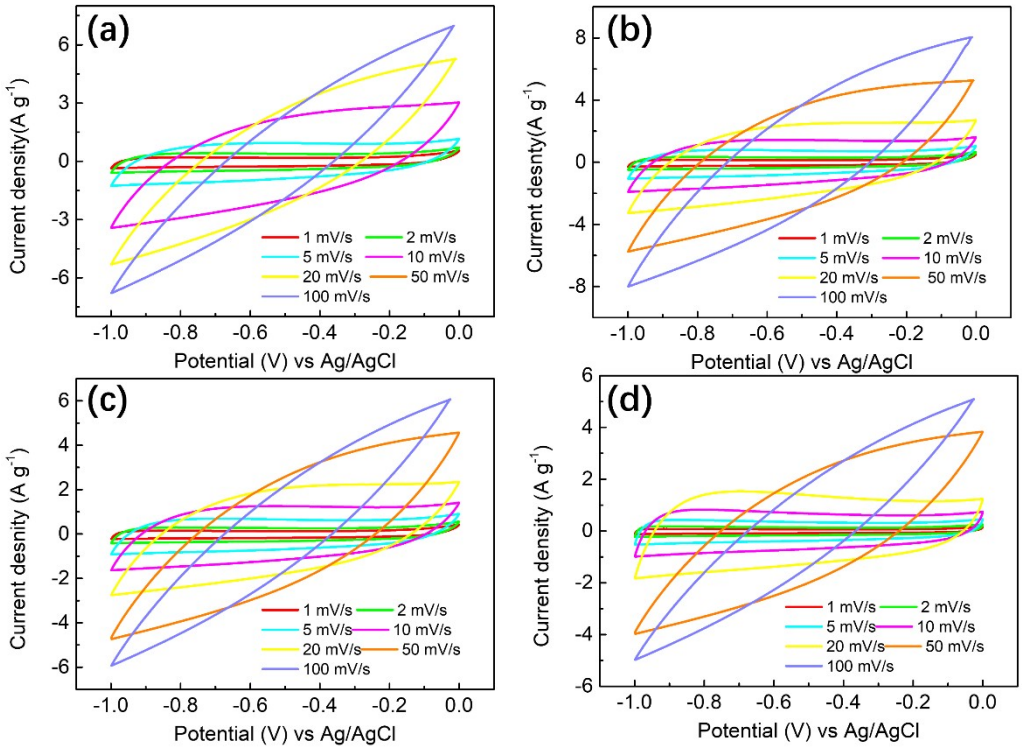

Fig. S13 CV curves of (a) DWCM-1-800 electrode, (b) DWCM-1-900 electrode, (c) DWCM-1-1100 electrode, and (d) DWCM-1-1200 electrode in 6 M KOH solution at different scan rates.

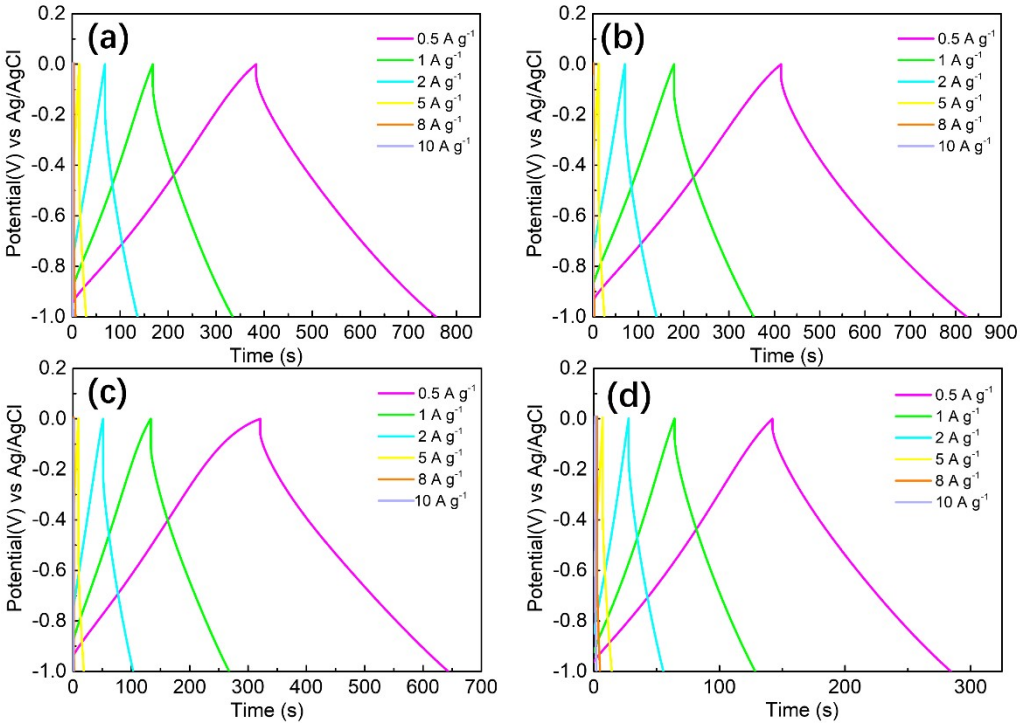

Fig. S14 GCD curves of (a) DWCM-1-800 electrode, (b) DWCM-1-900 electrode, (c) DWCM-1-1100 electrode, and (d) DWCM-1-1200 electrode at different current densities.

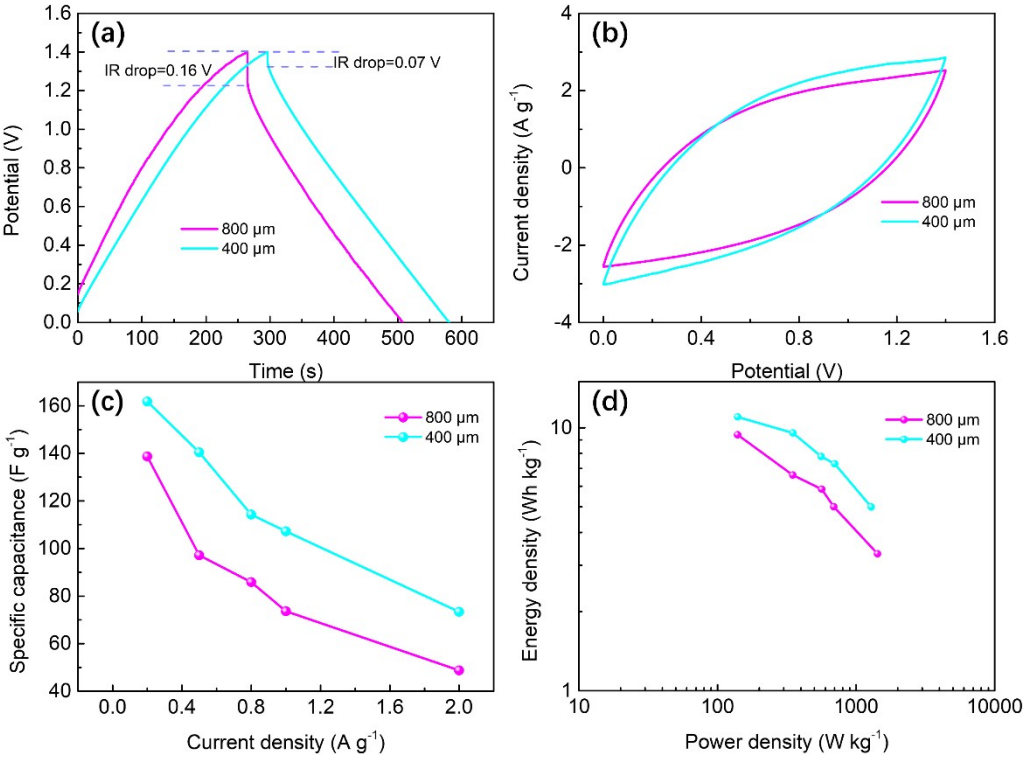

Fig. S15 (a) GCD curves of DWCM-1-1000 based SC with various thickness. (b) CV curves of DWCM-1-1000 based SC with various thickness. (c) The specific capacitance of DWCM-1-1000 based SC with various thickness at the current densities from 0.2 to 1 A g^{-1}. (d) The Ragone plots of DWCM-1-1000 based SC with

various thickness.

Table S1 Comparison of electrochemical performance of various powders and membrane carbon based symmetric supercapacitor

Material	Form	C_a (F g^{-1})	Cycling stability	Ref.
PAC-4	Powders	43 (0.5 A g^{-1})	96% (10000 cycles)	[S1]
SHPC-3	Powders	62 (0.5 A g^{-1})	93.3% (12500 cycles)	[S2]
HPC-2	Powders	68.3 (1 A g^{-1})	86.2% (10000 cycles)	[S3]
ABC-900	Powders	78.8 (0.5 A g^{-1})	92.1% (10000 cycles)	[S4]
LB-900	Powders	25 (1 A g^{-1})	83% (5000 cycles)	[S5]
TCNF	Powders	27.1 (0.2 A g^{-1})	94.5% (20000 cycles)	[S6]
CLCF	Powders	41 (1 A g^{-1})	90% (5000 cycles)	[S7]
CNBC	Powders	50 (1 A g^{-1})	97% (5000 cycles)	[S8]
PGBC	Powders	48.1 (0.2 A g^{-1})	84% (5000 cycles)	[S9]
C-800	Powders	35 (1 A g^{-1})	97% (1000 cycles)	[S10]
CHNS	Powders	64 (1 A g^{-1})	94% (6000 cycles)	[S11]
P-CNF	Powders	25 (1 A g^{-1})	94% (2000	[S12]

			cycles)	
CNF	Powders	37 (0.2 A g^{-1})	81.1% (10000 cycles)	[S13]
LCM	Membrane	193.7 (1 A g^{-1})	96.9% (100000 cycles)	[S14]
CDCM	Membrane	150 (1 A g^{-1})	90% (20000 cycles)	[S15]
DWCM-1-1000 (800 μm)	Membrane	138.3 (0.2 A g^{-1}) 97.1 (0.5 A g^{-1}) 85.9 (0.8 A g^{-1}) 73.6 (1 A g^{-1}) 48.8 (2 A g^{-1})	98% (20000 cycles)	This work
DWCM-1-1000 (400 μm)	Membrane	161.8 (0.2 A g^{-1}) 140.4 (0.5 A g^{-1}) 114.3 (0.8 A g^{-1}) 107.2 (1 A g^{-1}) 73.4 (2 A g^{-1})	98% (20000 cycles)	This work

Supplementary References

[S1]M. Rajesh, R. Manikandan, S. Park, B. C. Kim, W. J. Cho, K. H. Yu, C. J. Raj, Pinecone biomass‐derived activated carbon: the potential electrode material for the development of symmetric and asymmetric supercapacitors, Int. J. Energy Res. 2020, 44, 8591-8605.

[S2]L. Peng, Y. Liang, H. W. Dong, H. Hu, X. Zhao, Y. J. Cai, Y. Xiao, Y. L. Liu, M. T. Zheng, Super-hierarchical porous carbons derived from mixed biomass wastes

by a stepwise removal strategy for high-performance supercapacitors, J. Power Sources 2018, 377, 151-160.

[S3]L. L. Qiang, Z. G. Hu, Z. M. Li, Y. Y. Yang, X. T. Wang, Y. Zhou, X. Y. Zhang, W. B. Wang, Q. Wang, Hierarchical porous biomass carbon derived from cypress coats for high energy supercapacitors, J. Mater. Sci. Mater. Electron. 2019, 30, 7324-7336.

[S4]G. X. Zhang, Y. M. Chen, Y. G. Chen, H. B. Guo, Activated biomass carbon made from bamboo as electrode material for supercapacitors, Mater. Res. Bull. 2018, 102, 391-398.

[S5]D. S. Torres, R. R. Rosas, M. J. V. Romero, J. R. Mirasol, T. Cordero, E. Morallón, D. C. Amorós, Asymmetric capacitors using lignin-based hierarchical porous carbons, J. Power Sources 2016, 326, 641-651.

[S6]W. B. Kang, L. Zeng, S. W. Ling, C. Z. Lv, J. F. Liu, R. X. Yuan, C. H. Zhang, Construction of CoO/Co-Cu-S hierarchical tubular heterostructures for hybrid supercapacitors, Adv. Funct. Mater. 2021, 31, 2102184.

[S7]Y. Cheng, L. Huang, X. Xiao, B. Yao, L. Yuan, T. Li, Z. Hu, B. Wang, J. Wan, J. Zhou, Flexible and cross-linked N-doped carbon nanofiber network for high performance freestanding supercapacitor electrode Nano Energy 15 (2015) 66-74.

[S8]X. Hao, J. Wang, B. Ding, Y. Wang, Z. Chang, H. Dou, X. Zhang, Bacterial-cellulose-derived interconnected meso-microporous carbon nanofiber networks as binder-free electrodes for high-performance supercapacitors, J. Power Sources 352 (2017) 34-41.

[S9]Y. Gong, D. Li, C. Luo, Q. Fu, C. Pan, Highly porous graphitic biomass carbon as advanced electrode materials for supercapacitors, Green Chem. 19 (2017) 4132-4140.

[S10] A. Gopalakrishnam, S. Badhulika, Ultrathin graphene-like 2D porous carbon nanosheets and its excellent capacitance retention for supercapacitor J. Ind. Eng. Chem. 68 (2018) 25.

[S11] P. Schlee, O. Hosseinaei, D. Baker, A. Landmér, P. Tomani, M. J. Mostazo-López, D. Cazorla-Amorós, S. Herou, M.-M. Titirici, From waste to wealth: from

kraft lignin to free-standing supercapacitors, Carbon 145 (2019) 470.

[S12] Y. Liu, J. Zhou, L. Chen, P. Zhang, W. Fu, H. Zhao, Y. Ma, X. Pan, Z. Zhang, W. Han, E. Xie, Highly flexible freestanding porous carbon nanofibers forelectrodes materials of high-performance all-carbon supercapacitors, ACS Appl. Mater. Interfaces 2015, 7, 23515.

[S13] Q. Li, W. Xie, D. Liu, Q. Wang, D. He, Nitrogen and oxygen co-doped carbon nanofibers with rich sub-nanoscale pores as self-supported electrode material of high-performance supercapacitors, Electrochim. Acta 222 (2016) 1445.

[S14] J. W. Liu, S. X. Min, F. Wang, Z. G. Zhang, High-performance aqueous supercapacitors based on biomass‐derived multiheteroatom self-doped porous carbon membranes, Energy Technol. 8 (2020) 2000391.

[S15] J. W. Liu, S. X. Min, F. Wang, Z. G. Zhang, Biomass-derived three-dimensional porous carbon membrane electrode for high-performance aqueous supercapacitors: An alternative of powdery carbon materials, J. Power Sources 466 (2020) 228347.